Electrostatic interaction in BIAcore binding studies: A cause for anomaly

Nonavinakere Seetharam Srilatha and Gundlupet Satyanarayana Murthy*

Department of Molecular Reproduction, Development and Genetics, Indian Institute of Science, Bangalore 560 012, India

Sensograms of human chorionic gonadotropin–monoclonal antibody (hCG–MAb); ligand–ligate binding in the BIAcore were analysed. Surface-bound MAb in 0.1 M phosphate buffer was unaltered by the concentration of MAb (C_{MAb}) as well as pH of the sensogram. Surprisingly, at 0.01 M phosphate buffer concentration surface-bound MAb markedly decreased (300%) at pH 9. At low ionic strength Bovine Serum Albumin (BSA), a nonspecific protein, bound to the uncoupled (control channel) chip at pH 5, but not at 7. BSA so bound did show a dissociation profile like MAb, with fast and slow dissociating components. Binding of BSA to the chip at low ionic strength clearly established the presence of salt-dependent interaction between the protein and chip matrix. A model is proposed which rationally explains, on the basis of electrostatic interaction, the association and dissociation anomalies often encountered in the BIAcore sensograms.

Keywords: BIAcore, human chorionic gonadotropin, matrix–ligate interaction, monoclonal antibodies.

INVESTIGATIONS on protein–protein interactions are fundamental to biology, as they form one of the key reactions for eliciting specific biological response. Such interactions are complex with contributions coming from electrostatic, hydrophobic, hydrogen bond, van der Waals interactions, etc.[1,2]. Study of the equilibrium conditions (equilibrium constant K_A) of reactions is ambiguous, as K_A consists of two components, namely constants of dissociation (k_{-1}) and association (k_{+1}), K_A being k_{+1}/k_{-1}. Thus for a meaningful study real-time kinetics offers advantages over simple equilibrium kinetics. Study of the real-time interaction has been automated and BIAcore has been extensively employed for such studies[3–5]. Our studies showed that the BIAcore sensogram provides accurate data and the equipment has the precision to quantify 20–100 Response Units (RU) within 1% error against a background[6] of 15,000 RU. Utilizing this advantage we have shown that the reaction in a BIAcore chip is complex and proposed a hypothesis that the complex formed on the chip sterically blocks the transport of the antibody through the surface of the chip, leading to complex binding data[6]. An additional observation was that the protein bound could not be dissociated completely even after extended periods of washing, which remained unexplained. In the following we have investigated the effect of pH and salt on the association/dissociation characteristics of human chorionic gonadotropin–monoclonal antibody (hCG–MAb) interaction and offer a rational explanation for the non-dissociation of bound protein in the BIAcore. We also show that the kinetic data obtained should be interpreted with caution, taking into consideration the isoelectric point of the proteins under study.

*For correspondence. (e-mail: gundlupetmur@indiatimes.com)

Materials and methods

Preparation and characterization of the hCG[7] and their MAbs[8] have already been reported. Coupling of the hCG to the biosensor chip was done using CM5-chip by the method suggested in the manual. All sensograms were run at a flow rate of 100 µl/min to bring the reaction into pseudo first-order kinetics. Analysis of the sensograms was done as described earlier[6]. Briefly, the initial part of the sensogram (0–50 s) was fitted into a single exponential fit using the Graph Pad Prism program, taking the initial reading of the sensogram by extrapolation to zero time. Both surface binding capacity, Y_{max} and k_{+1} were obtained from the fit. Accuracy of the fit was found to be ±5%. Effect of salt on the sensogram was studied in 0.01 M phosphate (PO_4) buffer at different pH values using 0.5 M sodium chloride.

Acetylation of MAb was carried out using acetic anhydride by the standard procedure[7]. Extent of acetylation was >95% as measured by the reduction of colour developed with picryl sulphonic acid before and after acetylation[8].

Results

Figure 1 is a representative sensogram analysed using the graph pad prism program, fitting the points to the first-order exponential equation. The best fit was seen for the range 0–35 s, with minimum standard error in Y_{max} and k_{+1} (Table 1). These parameters were measured within 5% accuracy. They are the surface-bound MAb (Y_{max}) and the association constant (k_{+1}) with the surface-bound hCG. Each sensogram was analysed as above to obtain the kinetic parameters Y_{max} and k_{+1}.

Effect of hCG immobilization on Y_{max} (MAb-bound) was carried out by measuring Y_{max} of chips with different quantities of immobilized hCG (Table 2). The Y_{max} obtained for an MAb depended on the total amount of hCG immo-

bilized (column 2 vs 5 in all rows), but was independent of the concentration of the MAb used in the sensogram for the same chip (columns 2, 5 and 9). However, within a chip the total MAb bound at 300 s (RU_{300}) marginally increased with higher concentration of MAb (columns 3, 6 and 10), and identified the presence of MAb bound to hCG in regions interior to the surface. The reduction in the second rate constant can be easily ascribed to the diffusion factor, the linear dextran chains preventing MAb to diffuse freely into the chip through sterical blocking. The above concept is in conformity with the observation that MAb concentration increased the second binding (as seen by the total binding at 300 s) with the same Y_{max} (columns 4, 7 and 11).

Our earlier data on the real-time kinetics using radiolabelled hCG and immobilized MAb (on nitrocellulose discs) had shown that the rate constants changed with salt concentration significantly, enabling us to investigate the mechanism of the hCG–MAb interaction[9,10]. Similar studies were attempted using the BIAcore, wherein the concentration and pH of the buffer were changed. Figure 2 is a representative sensogram. The parameters Y_{max} and k_{+1} at different pH values and salt concentrations are presented in Table 3. Y_{max} and k_{+1} remained unaltered in high salt concentration (columns 2 and 3) and indicated that the extent of the primary reaction indexed by Y_{max} and k_{+1} is unchanged by pH. However, when the salt is removed from the reaction medium, the association reaction fitted to an exponential binding above pH 7.5 (columns 4 and 5). Y_{max} decreased remarkably as pH increased from 7.5 to 9.5. There was a corresponding increase in the rate constant (k_{+1}) and at 9.5 (column 5, row 5) exceeded the k_{+1} obtained in the presence of the salt (column 3). However, at lower pH (<7.0), the sensogram failed to fit into an exponential pattern, though binding markedly increased.

The rates determined present an average rate of interactions at each layer, and greater the depth of the diffusion, greater will be the heterogeneity and Y_{max}. Greater Y_{max} brings down the k_{+1} due to diffusion factor associated with the reaction occurring at the deeper layers of the chip. Hence at 9.5 the diffusion is much less than at lower pH, resulting in decreased Y_{max} with concomitant increase in k_{+1}. Thus the interaction between the matrix and the MAb at low ionic strength is a weak electrostatic interaction. This can be attributed to two sources. The first is that the pH alters the charges on the proteins (because of their isoelectric point), and second, the charge status of the matrix is altered by pH. The first possibility fails to explain the nonlinear interaction at pH 6.5 and below, and changes in Y_{max} observed between pH 9.5, 8.5 and 7.5. The second possibility is likely for the following reasons. The CM5-chip has a large number of carboxyl groups attached to the matrix. These groups at pH above 5.5 are

Table 1. Optimization of curve-fitting parameter

No. of points chosen (time range in s)	Y_{max} ± standard error (RU)	Y_{max} range (95% confidence) (RU)
4 [0–15]	351 ± 15.4	290–423
5 [0–25]	372 ± 5.4	355–389
6 [0–35]	361 ± 3.9	350–372
7 [0–45]	374 ± 5.5	360–389

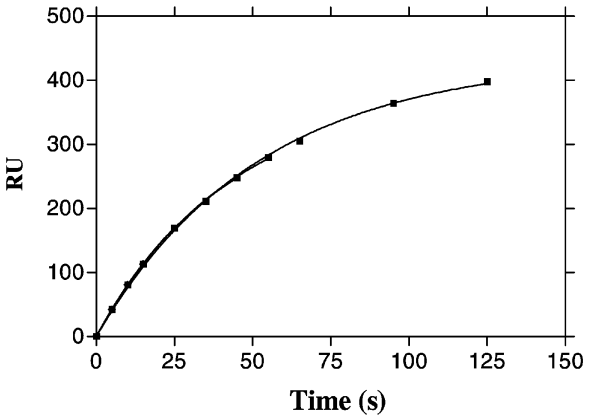

Figure 1. Sensogram of VM11 binding to hCG immobilized chip at pH 6.5 in 0.1 M phosphate buffer.

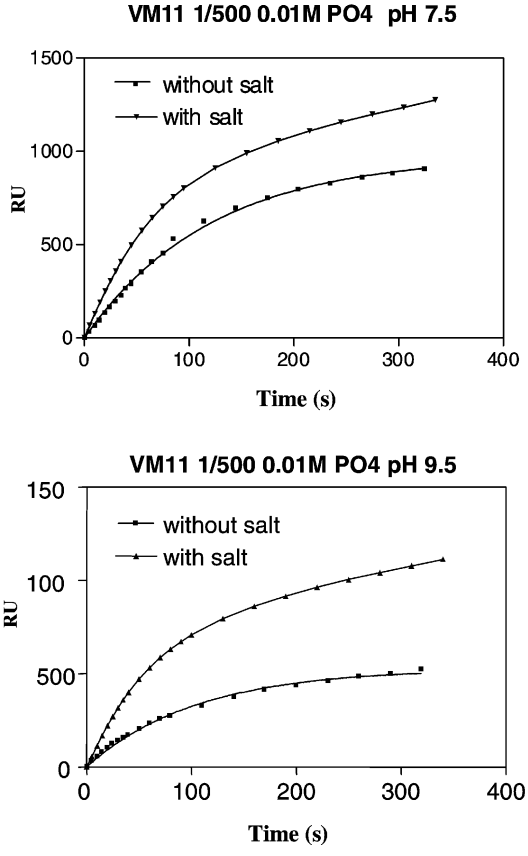

Figure 2. Sensograms obtained for binding of VM11 to hCG in BIAcore at two representative pH values of 7.5 (top panel) and 9.5 (lower panel) in the presence and absence of 0.5 M sodium chloride in 0.01 M phosphate buffer.

Table 2. Y_{max} measurement with varying amount of hCG immobilization

	VM10 (300 RU)**			VM10 (72 RU)**				VM11 (1200 RU)**		
a/s dilution	Y_{max}	RU_{300}	RU_{300}/Y_{max}	Y_{max}	RU_{300}	RU_{300}/Y_{max}	a/s dilution	Y^*_{max}	RU_{300}	RU_{300}/Y_{max}
1/200	271	392	1.45	107	155	1.45	1/2000	280	453	1.73
1/300	279	372	1.33	110	145	1.32	1/3000	300	393	1.45
1/400	276	350	1.27	103	132	1.28	1/4000	285	337	1.18

*Data obtained for VM11 MAb in 0.1 M phosphate buffer pH 7.5.
**Values present hCG coupled to the chip.

Table 3. Association rate constant of MAb VM11 in BIAcore

	0.01 M PO_4 with 0.5 M NaCl		0.01 M PO_4 without 0.5 M NaCl	
pH	Y_{max} [RU]	k_{+1}	Y_{max} [RU]	k_{+1}
5.5	1124	0.01210	Very high	–
6.5	1142	0.01495	Nonlinear	–
7.5	1168	0.01226	974	0.00829
8.5	1099	0.01145	687	0.01071
9.5	1090	0.01163	248	0.01753

Table 4. Binding of MAb and acetylated MAb to biochip

	Control VM11 (1/500)		Acetylated VM11 (1/50)	
pH	0.10 M	0.01 M	0.10 M	0.01 M
5.0	–	9415	65	–5
5.5	3686	7479	24	0
6.0	171	4315	16	0
6.5	0	1367	16.6	0

present as negative charges and hence capable of interacting with positively charged molecules. At high salt concentration, these charges interact with the buffer cations and do not affect the immunochemical interaction between the immobilized hCG and the MAb. However, in the absence of the salt, the charged carboxyl groups of the matrix interact with the charged protein (MAb in this case) affecting the kinetics of the interaction. Considering that the pH of the MAb is ~7 (IgG1-type), it is possible that the electrostatic interaction will play a part below pH 7, since at lower pH values, MAb will carry a positive charge and hence interact with the negative charges of the matrix.

This hypothesis was checked by the ability of acetylated MAb to bind to the control chip (Table 4). Though binding of VM11 was satisfactory (columns 2 and 3), that of acetylated VM11 was insignificant (columns 4 and 5). Binding of MAb increased to >200% in the absence of salt (column 2 and 3). However, in the case of acetylated MAb, binding in the absence of salt was insignificant (columns 4 and 5). This suggested a role for positive charges (*e*-lysine groups) in the binding. Acetylation of MAb would result in the protein having a lower isoelectric point and hence less positive charges at pH 6.5, consequently resulting in repulsion of the acetylated MAb (charged negatively) from the surface of the chip, and in poor binding.

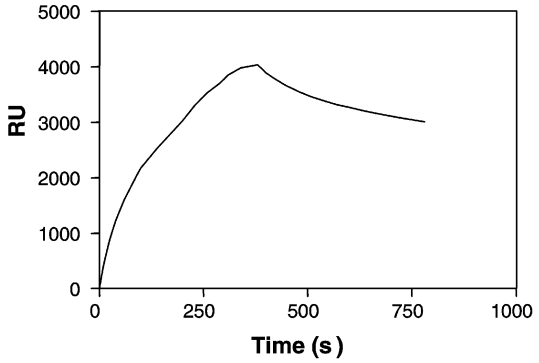

Figure 3. Binding of BSA to control chip. Conditions of binding were pH 5.0, 0.1 M phosphate buffer and BSA concentration of 10 µg/ml.

Table 5. Association and dissociation of BSA to hCG-coupled and control chip in phosphate buffer pH 5.0

Chip used	Salt concentration (M)	Association at 300 s (RU)	Dissociation at 450 s (RU)
hCG chip	0.10	3100	900 (29%)
hCG chip	0.01	3582	365 (10.2%)
Control chip	0.10	4200	924 (22%)
Control chip	0.01	5377	507 (9.4%)

Further evidence was obtained for the hypothesis by the binding of BSA to the control channel of the BIAcore chip in 0.1 M phosphate buffer pH 5 (Figure 3 and Table 5). The observation that BSA bound to the chip clearly demonstrated that the reaction is through the charges on BSA (pK_I is 5) and the matrix (pK_A of carboxyl group 4.5). Bound protein dissociated minimally on prolonged washing (Figure 3 and Table 5). The extent of dissociation that occurred at 450 s was 22% in 0.1 M salt concentration (Table 5, column 4, rows 1 and 3), but was 10% in 0.01 M salt concentration (rows 2 and 4), and proved that salt facilitated the dissociation. Association data also showed that binding was faster at lower ionic strength, as measured by the initial rate of the reaction (slope between 0 and 10 s), confirming the reduction of k_{+1} by salt. Thus interaction between the chip and BSA is electrostatic in nature. Dissociation did not correspond to the first-order kinetics, and analysis of the initial part of the dissociation indicated it to be non-homogeneous. There was a slow leaching of the

BSA bound after the initial fast dissociation. However, at pH 6.5 binding of BSA to the chip was negligible (<20 RU; data not shown).

Analysis of the real-time reaction between BSA and the chip (both association and dissociation) is shown for sensograms obtained in 0.1 M buffer, pH 5 (Figure 4). The parameters Y_{max}, k_{-1} and k_{+1} could be obtained with good consistency when the initial part of the sensogram was analysed by the standard method (Table 6). The rate of binding was increased about 50% in 0.01 M salt, based on the initial reaction period (not shown). Dissociation of the BSA from the control chip (Figure 4, curve A) did not fit into an exponential pattern, implying complex dissociation kinetics. When the initial phase of dissociation was fitted into an exponential dissociation (curve B), the result suggested additional dissociation/s with lower apparent rate constant/s (curve C). While the maximum dissociation possible by the fit of the early points of dissociation recorded Y_{max} of 600 ± 2 RU, by 450 s as much as 900 RU had been released. The profile was similar to the one seen in many other dissociation systems discussed earlier[4,6]. Y_{max} of 600 RU represents the MAb easily dissociated, probably bound to the chip at the surface (low electrical charge density) while the later dissociations observed are the ones buried in the gel and hence held back by the presence of negative charges around (from the carboxyl groups).

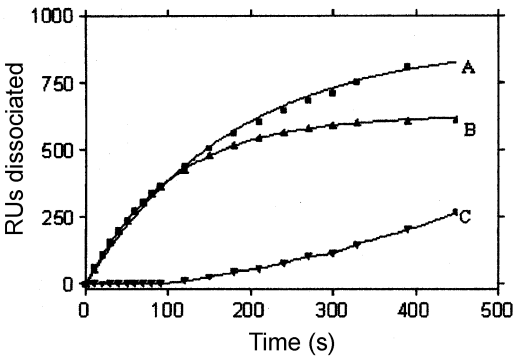

Figure 4. Dissociation of BSA from the chip at pH 5. A, B and C present the total dissociated, the theoretical plot for a first-order dissociation using the initial part of dissociation and slow dissociation observed [A–B] in the dissociation profile. The association was carried out at pH 5.0 in 0.1 M phosphate buffer. The total dissociation observed was 900 RU, of a total of 3100 RU bound at 300 s binding. Y_{max} for association and dissociation were 1500 and 633 RU respectively (Table 5).

Table 6. Real-time kinetics analysis of BSA in BIAcore

Chip	Salt concentration (M)	Association		Dissociation	
		Y_{max} [RU]	k_{+1}	Y_{max} [RU]	k_{-1}
hCG chip*	0.10	1500	0.017	633	0.00943
Control chip	0.10	2800	0.015	680	0.00970

*This is a chip to which 1200 RU of hCG was immobilized.

Discussion

Important observations of the above investigations were (a) Y_{max} and k_{+1} were independent of pH at high ionic strength, but varied with pH at low ionic strength. (b) Modification of charges on the ligate (MAb) reduced binding to the chip. (c) BSA bound nonspecifically to the chip at pH below 5.5. Added to these is the earlier observation that the binding and dissociation follow a complex kinetics in the BIAcore, and the MAb bound to the hCG-immobilized chip is not dissociated[6]. In the following we propose a model whereby the anomaly in the BIAcore sensograms is explained on a rational basis.

The model proposed is based on the valid assumptions (*BIAcore Manual*) that the chip consists of 2% linear dextran, and the volume[11,12] of the chip is 60 nl. It is assumed for convenience that the dextran chain is linear and that the chains are arranged linearly along the three axes. Representative example of the chip is as shown in Figure 5. The vertices in Figure 5 represent the boundary of the chip (assumed to be a perfect cube for the convenience of calculations), with each line indicating the dextran chain. Under these conditions, the distance between the dextran chains can be obtained (see Appendix).

Thus the chip is assumed to consist of a large number of smaller unit cells of dimension $100 \times 100 \times 100$ Å, arranged uniformly as in a crystal as shown in Figure 5 *a*. Each unit cell (Figure 5 *b*) will have a side of 100 Å, and hence in the CMS-chip the number of carboxyl groups on each side of the unit cell will be about 20 (each hexamer consists of a carboxyl group; *Handbook of BIAcore*, p. 3–3). Thus each unit cell will have a potential cube of 20 charged residues on each side of the cube, with a possible diffu-

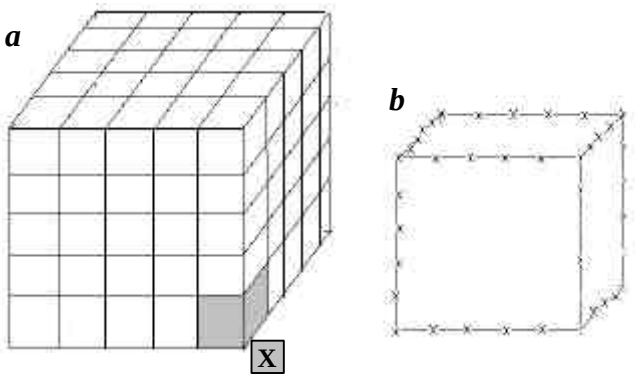

Figure 5. ***a***, Diagrammatic representation of theoretical projection of strands of the dextran polymer chain in the biochip. Theoretical arrangement of the chains is presented with each line representing the strand in *X*, *Y* and *Z* directions. Intersection of the strands does not present a chemical bonding between the two strands, but a spatial proximity. ***b***, Diagrammatic representation of a unit cell X in (***a***): Each line represents a linear strand of dextran polymer, with X presenting the carboxyl group attached to the polymer chain. The length of a unit cell is 100 Å, with carboxyl groups (*x*) at distances of about 5–7 Å. A total number of 200 carboxyl groups could be present around a cell, assuming that each hexamer is activated with a carboxymethyl group.

sion of proteins into this cube, unless its size is more than that of the surface of the unit cell. This is a simplified projection of the unit cell structure. Imperfection of the assumption that the dextran is a linear chain and aligned parallel will bring sufficient changes in the dimensions of each unit cell in all the surfaces, and hence the 100 Å distance provided is only a notional approximation, with large variations. Hence, in reality, the cell consists of unit cells of different dimensions and shapes, with an average length of 100 Å and an average of 200 carboxyl groups around each unit cell.

The model proposed explains all the observations listed in the beginning on a rational basis. Consistent Y_{max} at varying pH (0.1 M buffer), decrease in Y_{max} with increase in pH (0.01 M buffer) as well as the increase in the k_{+1} at pH 9.5 have already been explained earlier. That this effect is due to the electrostatic interaction has also been demonstrated by the observation that acetylation of MAb resulted in a large reduction of binding at all pH values (Table 4).

The surface of the chip consists of non-uniform unit cells aligned randomly. Cell surfaces which have a dimension of more than $[200\ Å]^2$, can become a region of diffusion for MAb (diameter 140 Å). Surface cells which have a unit length >50 Å allow hCG to diffuse. Thus during immobilization, hCG is bound to all unit cells which are above $[50\ Å]^3$. Thus the hCG bound will have three populations, one easily accessible to MAb (bound at the surface), the second buried in the interior not easily accessible, and the third not accessible to MAb. The hCG bound at the surface of the chip is the potential point of interaction because of its accessibility. Thus the chip has populations of hCG bound at different depths, projecting heterogeneity of binding despite identical chemical reaction. Reduction in the apparent rate of reaction in the second phase is due to the rate-determining diffusion process. Quantitative data on the binding of MAb to chips for which different amounts of the hCG was bound (Table 1), show that only a fraction of the hCG was bound at the surface (30% for 72 RU and 25% for 300 RU for VM10 and 14% for VM11 as seen by Y_{max}). Excess hCG coupled is sent to regions not accessible to MAb (hCG has a diameter of 38 Å and MAb 140 Å), as seen by the same Y_{max} for 300 and 1200 RU-coupled chips (Table 2, columns 2 and 9). Thus the differential accessibility of the hCG to the ligate solution gives a complex kinetic pattern for the association. On the same basis, its dissociation has complex patterns, as MAb has to diffuse first before being washed out. Hence the dissociation profile consists of surface-bound MAb (fast rate) and MAb bound in the interior of the chip (diffusion becomes rate-limiting).

Incomplete dissociation or presence of apparently non-dissociating complex in the matrix may arise out of the geometry of the MAb and that of the unit cell in which it is trapped. The dimension of the hCG–MAb complex is expected to span about 80 + 140 = 220 Å, and such a complex may be trapped by movement of the linear dextran chain within a unit cell, induced by electrostatic interaction between the negative charge on the unit cell and the positive charge of the protein trapping the complex sterically. Thus those molecules which fit snugly into a unit cell of dimension $[200–300\ Å]^2$, fail to dissociate due to sterical blocking induced by the hCG–MAb interaction. Observations that not all surface-bound MAb is dissociated (Figure 3, Table 5), and the earlier observation that the MAb bound to immobilized hCG did not dissociate, but the hCG bound to this immobile hCG–MAb complex (located at the surface) dissociated completely (Figure 3 in ref. 6), gives credibility to the hypothesis that the movement of the dextran fibres through electrostatic interaction holds the primary hCG–MAb complex, but the hCG bound to the complex (hence exposed and not constrained by the dextran chains) was completely dissociated with a single k_{-1}.

The unit cell has enough charges in the CM5-chip at pH above 5. The MAbs have pK_A around 7, and hence at pH < 7, the protein itself is likely to have positive charges. That Y_{max} and k_{+1} values did not change in 0.5 M salt, clearly suggests that the charges in the chip or in the protein had little role in the immunochemical interaction. However, low salt concentration allows electrostatic interaction between the hCG and MAb to influence the kinetics giving rise to changes in Y_{max} and k_{+1} (Table 2). Data obtained with acetylated MAb justify the conclusion (Table 4). That the reaction seen between pH 5 and 6 is not connected with any immunological property of the ligand–ligate becomes clear from the binding of BSA to the chip (Figure 4, Tables 5 and 6). The isoelectric point of BSA is much lower than that of MAb and can be expected to have positive charges at pH 5. Increase in the binding seen between pH 6 and 5 clearly indicates that the reaction is mediated through the electrostatic interaction between the charged unit cells and BSA trapped in these cells. This is further justified by the observation that this increase in the binding is reduced significantly when the pH is increased to 6, as well as the observation that the binding is also reduced in the presence of the salt. Even under this condition, a large fraction of the BSA that did not dissociate suggests strong charge-mediated interaction. Association rate constants are not altered with native chip or hCG-coupled chip, indicating that surface binding of albumin is independent of any protein attached to the cell. The dissociation profile is again complex for the same reasons already explained earlier. It is also seen that dissociation is more in the presence of salt (Table 5).

Results presented above show that the reaction between MAb and hCG is more complex, and signify the importance of considering charged residues in the interpretation of the sensograms obtained. In most cases, high concentration of salt can take care of the weak interactions, but in cases where the charge density becomes more like in the BSA, electrostatic interactions may be too strong to be completely disrupted by high salt concentration (Table 6). Likewise, in chemical modification studies, those modification/s

that affect the charges and hence change the isoelectric point of the ligand (MAb in our studies) can alter the association constant. If the proteins involved have high pK_I, it would be better to run the sensogram at a pH close to or more than the pK_I. The data also indicate that even in cases where dissociation is minimal, association rates can be obtained with certainty using the initial part of the sensogram, as this part provides two important constants, namely Y_{max} and k_{+1}.

In conclusion, we have identified the reason for lack of dissociation of the hCG–MAb complex in the BIAcore. pH, ionic strength and isoelectric point of the ligand are important in the interpretation of the sensogram. Y_{max} and k_{+1} can be obtained with a 2–3 min sensogram, without any consideration for the apparent non-dissociating nature of the complex. However, it is important to note that the results will have to be evaluated giving due consideration to the electrochemical properties of the ligand, ligate and chip. A study of the interaction using the above-mentioned analysis quantitatively provides data for comparative studies, both in association and dissociation. However, kinetics studies of the reaction involving diffusion (slow binding) is far from easy at this point of time.

Appendix

Assumptions and rationale of the calculation are as follows.

1. The dextran chain is linear and the length of each polymeric unit of the hexamer is 6 Å.
2. The dextran chain is arranged in parallel lines in the matrix in *x*, *y* and *z* axis, and spread uniformly.
3. The total length of the chains is the sum of the individual lengths of the linear chains spread between the boundaries of the chip.
4. Total weight of the dextran in each chip is 1.2 µm. (2% dextran and volume of the chip is 60 nl).
5. It is assumed that the chip is a perfect cube.

Total weight of the dextran in the chip is 1.2 µg.

Molecular weight of each monomer in the dextran is 180.

Therefore, number of molecules of the monomer in 1.2 µg dextran = 3.7×10^{15}.

Length of each monomer unit is considered to be 5 Å.

Total length of the dextran chains should be $5 \times 3.7 \times 10^{15}$ Å = 18.5×10^{15} Å.

Volume of the chip = 60 nl.

1 ml = 1 cc [density of the chip material is taken as 1 g/cc] $[10^8]^3$Å^3.

1 µl = 10^{21}Å^3.

1 nl = 10^{18}Å^3.

60 nl = $[60 \times 10^{18}]$ Å^3.

Length of the chip assuming it to be a perfect cube will be $[60 \times 10^{18}]^{1/3}$Å^3 = 4×10^6 Å.

Number of dextran chains arranged in each chip will be $n^2 \times 3$, where n is the no. of parallel segments of the dextran on each face of the cube.

Total length (4×10^6 Å) of the dextran chain is assumed to be distributed equidistant, and hence the distance between the vertices (like between A and B, etc.) is $n^2 \times 3 \times 4 \times 10^6 = 18.5 \times 10^{15}$.

Therefore, $n^2 = 1.5 \times 10^9$ and hence $n = 4 \times 10^4$.

Length of the side of the chip (chip is assumed to be a cube) = 4×10^6 Å.

Therefore, distance between each strand of dextran = 100 Å $[\{4 \times 10^6\}/\{4 \times 10^4\}]$Å.

1. Tsumoto, K., Ogasahara, K., Ueda, Y., Watanabe, K., Yutani, K. and Izumi, K., Role of salt bridge formation in antigen-antibody interaction. Entropic contribution to the complex between hen egg white lysozyme and its monoclonal antibody HyHEL10. *J. Biol. Chem*., 1996, **271**, 32612–32616.
2. Sheinerman, F. B., Norel, R. and Honig, B., Electrostatic aspects of protein–protein interactions. *Curr. Opin. Struct. Biol*., 2000, **10**, 153–159.
3. Malmqvist, M., Biospecific interaction analysis using biosensor technology. *Nature*, 1993, **361**, 186–187
4. Lipschultz, C. A., Li, Y. and Smith-Gill, S., Experimental design for analysis of complex kinetics using surface plasmon resonance. *Methods*, 2000, **20**, 310–318.
5. Thomas, C. J. and Surolia, A., Kinetic analysis of the binding of Ulex europeas agglutinin 1 (UEA 1) to H-antigenic fucolipid. *Arch. Biochem. Biophys*., 2000, **374**, 8–12.
6. Ashish, B. and Murthy, G. S., Analysis of human chorionic gonadotropin-monoclonal antibody interaction in BIAcore. *J. Biosci*., 2004, **29**, 57–66.
7. Venkatesh, N., Nagaraja, G. and Murthy, G. S., Analysis of a conformation specific epitope of the alpha subunit of human chorionic gonadotropin: Study using monoclonal antibody probes. *Curr. Sci.*, 1995, **69**, 48–56.
8. Venkatesh, N. and Murthy, G. S., Immunochemical approach to the mapping of an assembled epitope of human chorionic gonadotropin: Proximity of CTP-*a* to the receptor binding region of the *b*-subunit. *J. Immunol. Methods*, 1997, **202**, 173–182.
9. Srilatha, N. S., Selvi, P. T. and Murthy, G. S., Epitope mapping from real time kinetic studies – Role of cross-linked disulphides and incidental interacting regions in affinity measurements: Study with human chorionic gonadotropin and monoclonal antibodies. *J. Biosci*., 2005, **30**, 359–370.
10. Ashish, B., Venkatesh, N. and Murthy, G. S., Structure function analysis: Lessons from human chorionic gonadotropin. *Indian J. Expt. Biol*., 2002, **40**, 434–447.
11. Murthy, G. S., Real time kinetic analysis of antigen-antibody interaction using solid phase binding: Transformation of hCG-monoclonal antibody complex. *Curr. Sci*., 1996, **71**, 981–988.
12. Hall, D. R., Cann, J. R. and Winzor, D. J., Demonstration of an upper limit to the range of association rate constants amenable to study by biosensor technology based on surface plasmon resonance. *Anal. Biochem.*, 1996, **235**, 175–184.

Received 25 May 2005; accepted 30 November 2005